Investigation of cadmium telluride grown by molecular-beam epitaxy using micro-Raman spectroscopy below and above the laser damage threshold

Sandeep Sohal,[1,a)] Madhavie Edirisooriya,[1] Thomas Myers,[1] and Mark Holtz[1,2]
[1]*Materials Science, Engineering, and Commercialization, Texas State University, San Marcos, Texas 78666*
[2]*Department of Physics, Texas State University, San Marcos, Texas 78666*

(Received 15 July 2018; accepted 29 August 2018; published 12 September 2018)

The effects of visible laser light on cadmium telluride (CdTe), grown by molecular beam epitaxy, are studied at low ($48\,\mu W/\mu m^2$) and high ($480\,\mu W/\mu m^2$) laser power densities using micro-Raman spectroscopy. The Raman spectrum of CdTe shows no notable change at low power density $\sim 48\,\mu W/\mu m^2$ for prolonged laser exposure. At higher power density $\sim 480\,\mu W/\mu m^2$, the Raman spectrum is significantly changed and strong Te-related peaks appear in the spectrum, even for short laser exposure times suggesting that photo-induced Te enrichment happens at the CdTe surface at high laser power density. The temperature rise is estimated from observed shifts in the Te and CdTe optical phonon peaks and modeled using finite-element simulations. At laser power $480\,\mu W/\mu m^2$, the CdTe exhibits a rise of ~44 °C above room temperature while the observed change in Te temperature is significantly higher, ~179 °C. The approach illustrates steps needed to establish the laser damage threshold for CdTe. *Published by the AVS.* https://doi.org/10.1116/1.5048526

I. INTRODUCTION

Raman spectroscopy is a powerful technique for investigating material properties of diverse semiconductors. Information available from these measurements includes material quality, stress, size effects, phonon-phonon processes, and structural phase. An exception to this broad applicability is several materials from the II-VI class, including cadmium telluride (CdTe),[1,2] ZnTe,[3] and CdZnTe.[4] Structural changes due to heating effects by above band gap laser excitation limit the applicability of the Raman measurements for studying these materials. Presumably, laser-induced degradation alters the material during the measurement, an effect that has received long-standing interest.[3–6] This undesirable effect limits the usefulness of Raman studies, for material analysis, as well as other optical techniques commonly using laser excitation, such as photoluminescence spectroscopy.

Surface damage has been reported at relatively high power density ($\sim 10^6\,W/cm^2 = 10^4\,\mu W/\mu m^2$) by observing tellurium-related peaks when measuring the Raman spectrum of CdTe.[7] Similar laser-induced Te peaks have been reported in ZnTe (Refs. 3 and 8) and CdZnTe (Refs. 4 and 5) materials. The Te Raman modes near 121 and 141 cm^{-1}, having A_1 and E symmetry, respectively, begin to appear in the Raman spectrum when the CdTe surface is illuminated, and their intensity grows with laser exposure time. Unfortunately, literature reports make difficult the determination of measurable laser power density applicable for studying the properties of CdTe without degrading the material. This is important due to the tradeoff between intensity needed for acceptable Raman signal and the onset of degradation. A combination of factors, such as surface properties of CdTe, laser power density, and laser exposure duration, is crucial to observe Te peaks in the Raman spectrum.[2]

Improvements in instrumentation make possible Raman measurements at low laser excitation power density to enable, among other investigations, application of this method to analysis of materials which are degraded by illumination.[9,10] We report micro-Raman studies of CdTe, grown by molecular beam epitaxy (MBE), at 48 and 480 $\mu W/\mu m^2$ power densities, and for different exposure times, using 532 nm laser excitation. MBE-grown CdTe is chosen for this study because it exhibits relatively narrow Raman features, is expected to be representative of single crystalline material, and has good surface properties. In this study, at low power, we do not observe Te peaks in the Raman spectrum of CdTe. However, at intensity $480\,\mu W/\mu m^2$, we observe the formation of Te-related Raman peaks which grow with continued exposure. Shifts observed in the Te and CdTe peak positions, at higher power density, allow us to estimate the optically induced temperature rise, which is significantly higher in the Te than in the CdTe.

II. EXPERIMENTAL DETAILS

CdTe was grown with 1-μm thickness on commercial (100)-oriented CdTe substrates using molecular beam epitaxy.[11] The sample has a low iodine doping concentration of $1 \times 10^{15}\,cm^{-3}$. The CdTe layer was grown under conditions optimized to produce near 1:1 stoichiometry of Cd and Te. X-ray diffraction rocking curve full width half maxima is 0.006° at 28.65-degree peak position as shown in Fig. S1 in the supplementary material.[27] The atomic force microscopy image shown in Fig. S2 (Ref. 27) and has root mean square surface ~1.32 nm. Micro-Raman measurements were performed at ambient room temperature using a commercial (Horiba LabRam HR) system in the backscattering geometry with instrument spectral resolution ~0.35 cm^{-1}. The 532-nm excitation was focused, and the Raman signal was collected with a 100× objective (NA ~ 0.90). The laser spot at sample

a)Electronic mail: Sandeep.Sohal@txstate.edu

surface was measured using the standard knife-edge method. The laser beam is described by a Gaussian function with estimated $1/e^2$ beam diameter $\sim 1\,\mu$m. The optical penetration depth of 532 nm excitation wavelength is ~60 nm in CdTe.[12] Therefore, the measurements emphasize near-surface properties. For establishing the temperature dependence of the CdTe longitudinal optical (LO) phonon energy, Raman measurements were conducted with the sample mounted to a controlled Peltier heating stage varied from room temperature up to 115 °C.

III. RESULTS AND DISCUSSION

Figure 1 presents Raman spectra of CdTe at power density $\sim 48\,\mu\text{W}/\mu\text{m}^2$ following different total laser exposure times. This is a generally low intensity for micro-Raman measurements. The spectrum in Fig. 1(a) was recorded for 1 min duration (integration time) beginning immediately upon exposure to the laser. The spectrum in Fig. 1(b) was recorded for 2 min after exposing sample for a total of 11 min duration. The spectrum in Fig. 1(c) was recorded for 5 min after exposing sample for 26 min, which includes laser exposure time of 1(a) and 1(b), ending after a grand total 31 min exposure. Each Raman spectrum exhibits the expected CdTe LO phonon peak at $166.8 \pm 0.4\,\text{cm}^{-1}$ based on fits using Lorentzian line shapes. In the Raman data in Fig. 1, no notable shift in LO phonon peak has been observed with laser exposure time. Furthermore, no additional features are seen in the spectrum related to the presence of excess Te. The result was checked elsewhere, as shown in Fig. S3 in the supplementary material,[27] on the sample with $48\,\mu\text{W}/\mu\text{m}^2$ laser exposure for a total of 80 min without observation of Te peaks in Raman spectrum. These results suggest that Raman measurements at this power density produce negligible optical damage to the sample and are therefore viable for materials analysis.

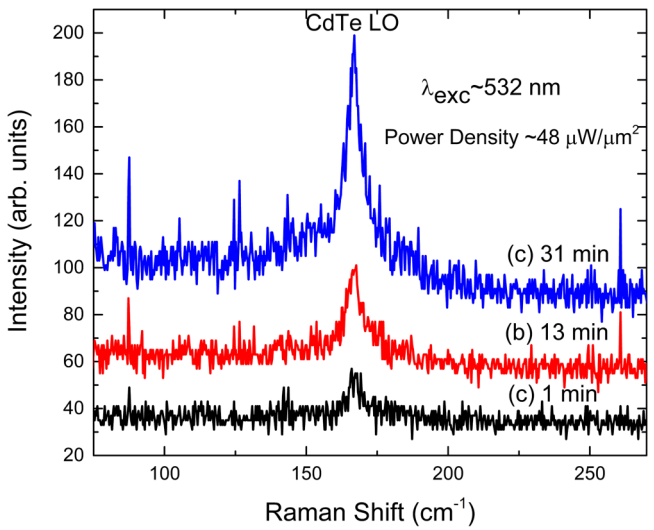

FIG. 1. Raman spectra of CdTe/CdTe (100) sample excited with 532 nm for different laser exposure times at power density $48\,\mu\text{W}/\mu\text{m}^2$. The CdTe LO phonon peak is observed. (a), (b), and (c) represent the Raman spectrum at 1, 13, and 31 min laser exposure time, respectively. Note integration time for (a)–(c) was different.

We subsequently raised the power density to $480\,\mu\text{W}/\mu\text{m}^2$, also for different exposure times, to help establish the onset of laser damage. Results are summarized in Fig. 2. A total of 25 sequential Raman spectra were recorded, each with 30 s acquisition time, for a grand total laser exposure time of ~750 s. We present representative Raman spectra in Fig. 2(a). For the early exposure times (~30 s), we observe the CdTe LO phonon at $166.6 \pm 0.5\,\text{cm}^{-1}$ and a very weak peak near $124.5\,\text{cm}^{-1}$ close to the baseline intensity. As the exposure duration continues to grow, intensity of the peak around $124.5 \pm 0.5\,\text{cm}^{-1}$ clearly increases and a new peak $\sim 141.4 \pm 0.5\,\text{cm}^{-1}$ appears in the spectra. These two peaks have been previously reported and are assigned to A_1 and E symmetry, zone-center phonons of crystalline Te.[4,5,13,14] From fits to the spectra, we observe a change in the peak position of CdTe LO phonon position. Although the variations are very small, the gradual trend observed in Fig. 2(b) shows a red shift with exposure duration. As discussed below, the observed red shift can be attributed to laser heating of the CdTe. The Te peaks are similarly examined. We summarize the A_1 and E peak positions and intensities, versus exposure time, in Figs. 2(c) and 2(d). The systematic red shifts similarly indicate gradual sample heating. The line widths of the phonon peaks studied do not show any trend with exposure time.

Figure 2(c) suggests that laser exposure time significantly affects the peak position and intensity of Te (A_1) Raman mode. The peak red shifts ($\sim 2\,\text{cm}^{-1}$) and grows in intensity with continued exposure time. Around 300 s exposure time, the Te peak begins to saturate in both position shift and intensity. A similar trend is observed in Fig. 2(d) for the Te (E) phonon, although the red shift is much smaller compared to the A_1 band. Saturation is similarly observed after 300 s exposure time. These data suggest denaturing of the CdTe surface due to laser heating and the formation of additional Te at the surface, as previously discussed by Soares and Do Carmo[2] and Soares *et al.*[7] We do not observe Raman bands in the 600–850 cm^{-1} range, related to TeO_x,[15] allowing us to rule out formation of tellurium oxides on the surface and its effects on Te peak during laser exposure time. We also do not observe any shift in Te peak position when checking at lower power density immediately following the high laser power density measurement and at the same laser spot. This result provides confidence that the observed shift in the Te phonon is attributable to temperature rise. Hawkins *et al.* observed laser-induced Te enrichment at the surface of CdZnTe at laser power density $\sim 6\,\mu\text{W}/\mu\text{m}^2$ (lower than the $48\,\mu\text{W}/\mu\text{m}^2$ used in our study).[4] The authors propose Te thermomigration as the cause behind the observed enrichment. However, they only observe Te-related features with no CdZnTe-related phonons,[4] suggesting that their starting material may have different surface properties than the CdTe investigated here. The temperature rise estimated in our study, as discussed later in this section, is below the melting point of Te arguing against thermal migration playing a significant role in our study.[16,17]

The Raman data may be used to estimate the local temperature rise in the CdTe and Te due to laser heating. We

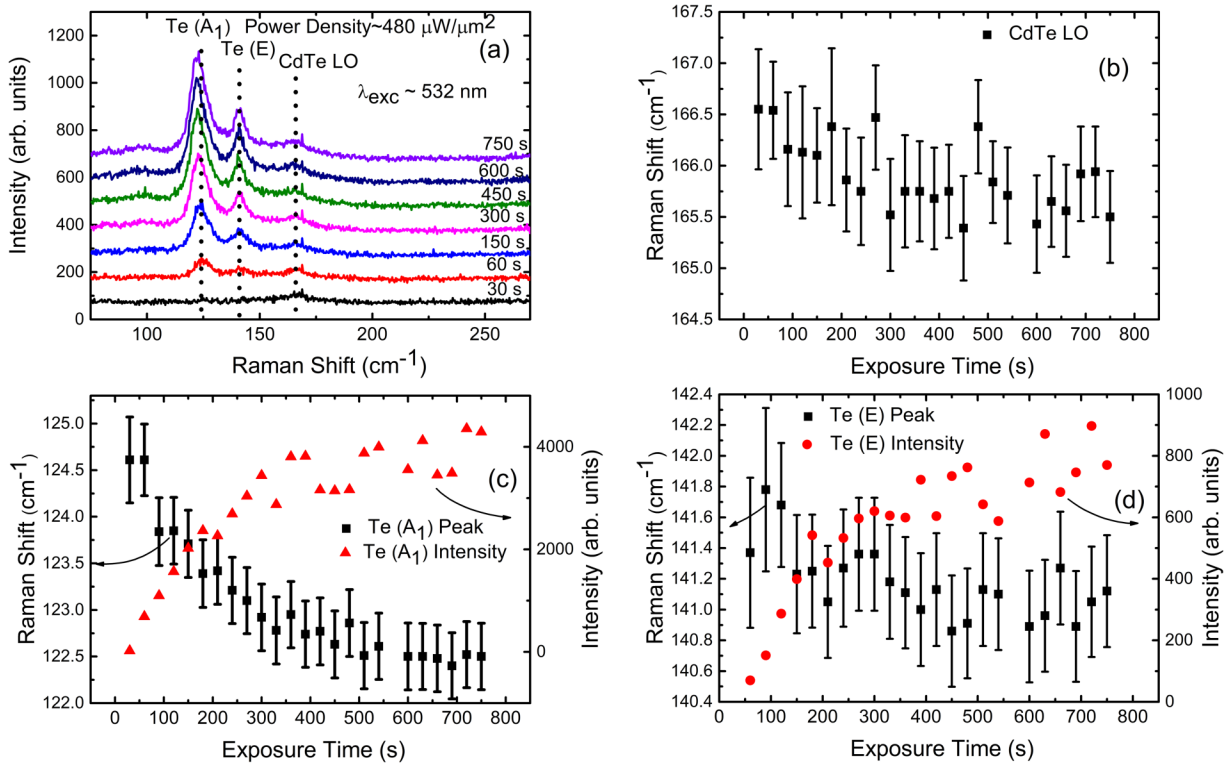

FIG. 2. (a) Micro-Raman spectra for different laser exposure times at power density 480 μW/μm^2. The dashed lines highlight the peak position of Te(A_1), Te(E), and CdTe LO phonons. (b) Raman shift of CdTe (LO) phonons vs exposure time. (c) Raman shift of Te (A_1) phonon (left-axis) (symbol: black square) and intensity (right-axis) (symbol: red triangle) vs exposure time. (d) Raman shift of Te(E) phonon (left-axis) (symbol: black square) and intensity (right-axis) (symbol: red circle) vs exposure time. The uncertainty in peak positions in (b–d) is based on instrument resolution (0.35 cm^{-1}) and uncertainty from fitting individual spectra.

calibrate the LO phonon energy by mounting the CdTe to a heating stage, to produce a known temperature rise, and measure the Raman spectrum at low excitation intensity. Peak position is shown in Fig. 3 from room temperature to $T = 115$ °C. For $k_BT > \hbar\omega_{LO}$, where k_B is the Boltzmann constant and $\hbar\omega_{LO} \sim 20$ meV is the LO phonon energy of CdTe,

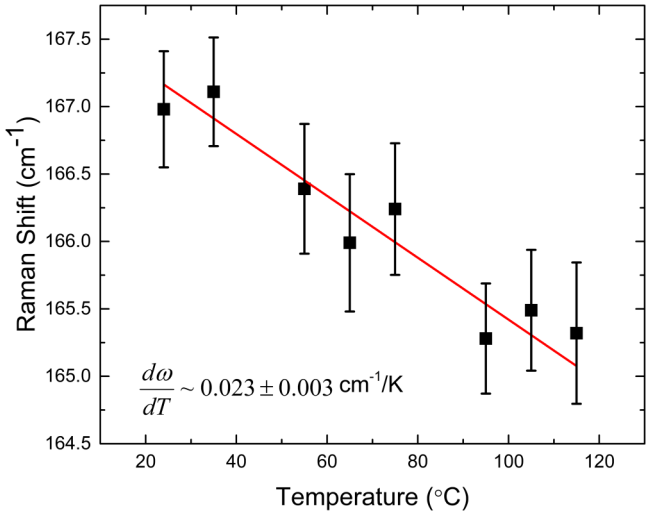

FIG. 3. Raman shift of CdTe LO phonon energy with temperature. The red line is a linear fit to data. The uncertainty in peak positions is based on instrument resolution (0.35 cm^{-1}) and uncertainty from fitting individual spectra.

the shift is approximately linear in temperature. The corresponding temperature range is >240 K so that data in Fig. 3 are within the linear range. A least-square linear fit to the data in Fig. 3 results in a phonon temperature coefficient of $d\omega/dT = -0.023 \pm 0.003$ cm^{-1}/K. The observed $\Delta\omega = -1$ cm^{-1} shift in the CdTe LO phonon corresponds to a local temperature rise of $\Delta T \sim 44$ °C. This is a rather modest temperature rise relative to the melting temperatures of CdTe (>1000 °C), Te (450 °C), and Cd (321 °C).[16,18,19]

We also gain insight from the temperature rise using the tellurium A_1 peak shift in Fig. 4. The temperature dependence of the A_1 phonon frequency has been reported by Hunsche *et al.* for crystalline Te in the 300–500 K range.[20] The phonon temperature coefficient is $d\omega/dT = -0.0118 \pm 0.0018$ cm^{-1}/K. The observed $\Delta\omega = -2.1$ cm^{-1} peak shift of the Te (A_1) with exposure time at power 480 μW/μm^2 corresponds to $\Delta T \sim 179$ °C local temperature rise.

It is interesting that the Te temperature rise is significantly greater than what is observed for the CdTe during high power laser exposure time in Fig. 4. This may be due to difference in properties of Te and CdTe. The high absorption coefficient of Te ($\sim 5 \times 10^5$ cm^{-1}),[21] compared to CdTe ($\sim 8 \times 10^4$ cm^{-1}) at 532 nm excitation wavelength,[12] results in more laser power absorbed by the Te when it is present at the surface as a thin film or as islands at the surface or within the near-surface region. One consequence of this scenario is that the initial composition of a CdTe sample plays

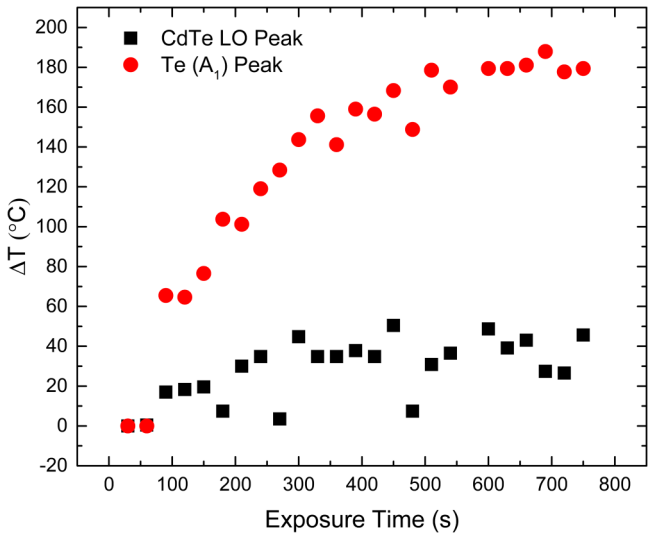

FIG. 4. Temperature rise vs exposure time for CdTe LO (symbol: black square) and Te phonons (symbol: red circle).

an important role in any laser-induced Te formation, which may explain diversity in reports of laser heating. Further, if the Te enriches due to laser exposure, the high optical absorption will increase the local heating of the Te relative to the CdTe. Our estimated temperature rise ~179 °C, based on Te phonon shift at higher laser power density, which is below the melting point of Te, suggests that Te thermal migration is not a possible cause for Te enrichment on surface. Another factor that may effectively enrich Te is Cd sublimation under laser illumination, a process which may occur around 200 °C.[22]

To examine laser heating at higher power density as a cause of the observed temperature rises, we also performed finite-element simulations using COMSOL MULTIPHYSICS. A custom three-dimensional simulation was carried out on a CdTe block 30 μm × 30 μm and thickness 10 μm. To simulate

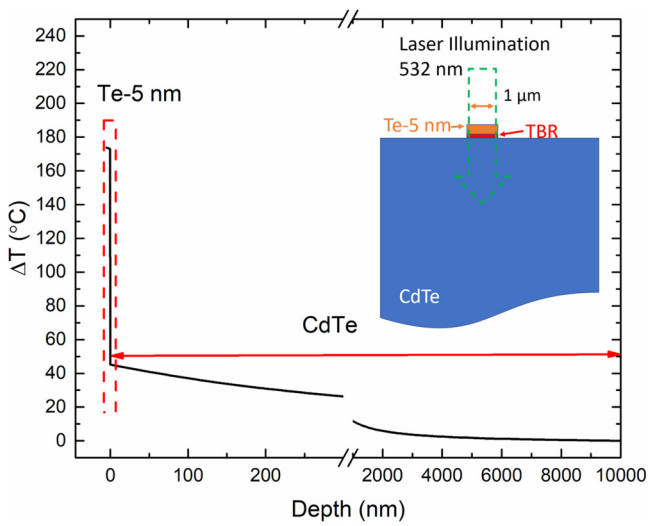

FIG. 5. Simulated temperature rise relative to room temperature vs depth. Dashed rectangle denotes near-surface region of interest. Inset depicts the simulated geometry. The TBR stands for thermal boundary resistance.

the Te, a thin layer with area ~1 μm^2 was produced on the surface of CdTe. We chose Te thickness value of ~5 nm, close to the excitation penetration depth (~10 nm) for Te. The observation of the Raman signal from CdTe, with prolonged laser exposure time in Fig. 2(a), also suggests that laser-induced Te thickness at the surface is not significantly greater than 10 nm. Simulations varying the Te thickness, between 1 and 10 nm, showed the resulting heating to be insensitive to the exact choice. Room temperature was taken as the ambient condition far from the laser spot in our simulations. The laser power was introduced across the Te area with a boundary heater source of power ~367 μW. This reduced power takes into account reflectance losses at the surface. We found that the simulated temperature profiles were not sensitive to the thermal conductivity of Te owing to it being very thin. We therefore use the literature value of 2 W/(m K).[23] Remaining parameters in the model were the thermal conductivity of CdTe and thermal boundary resistance (TBR) between the two materials. The simulated temperature rises in Te and CdTe were found to be sensitive to these two parameters. This simulation shows that asymmetric heating of the surface Te and CdTe is readily achieved, as seen in the simulated temperature profile of Fig. 5. To estimate the observed temperature rise in CdTe, we computed a weighted average of the depth-dependent temperature rise (ΔT) above ambient within the CdTe according to $\Delta T = \int \Delta T(x)\exp(-\alpha x)dx / \int \exp(-\alpha x)dx$, where $\Delta T(x)$ is the simulated temperature rise as a function of depth x in the CdTe and α is its optical absorption coefficient at wavelength 532 nm. The estimated $\Delta T = 44$ °C of CdTe is obtained when using thermal conductivity of 4 W/(m K) for CdTe; the temperature rise of 174 °C within the simulated Te layer was obtained with a TBR of ~3.5×10^{-7} m^2 K/W. The thermal conductivity of CdTe is lower than the accepted value ~7 W/(m K).[24,25] The authors in Ref. 24 suggest that lower crystalline quality and defects may reduce thermal conductivity in their comparative study of thermal properties of poly and single crystalline CdTe materials. In our study, we note that unpassivated CdTe, grown by MBE, is highly susceptible to near-surface defects. Furthermore, the value we obtain is for CdTe which has been denatured by the local laser heating. Both of these factors are expected to reduce the thermal conductivity of the CdTe. We find no reports of the TBR between CdTe and Te. The value obtained here is high in comparison to what has been generally reported for materials.[26] This suggests that the Te is in poor thermal contact with the CdTe.

IV. CONCLUSIONS

We have investigated the effect of laser power density on MBE-grown CdTe using micro-Raman spectroscopy. Raman spectra of CdTe were measured for different sequential laser illumination intervals at 48 and 480 μW/μm^{-2} power densities. Raman bands from Te begin to appear in the Raman spectrum of CdTe at higher power density 480 μW/μm^{-2}, whereas no Te peak is seen at 48 μW/μm^{-2} for prolonged laser exposure times. The presence of these Te bands in the

Raman spectra suggests degradation of the CdTe surface. We estimate the temperature rise with laser exposure time, at the higher intensity, based on shifts measured in the Te and CdTe phonon positions. It is interesting that the Te material experiences much greater temperature rise (up to ~179 °C from room temperature) compared to CdTe (~44 °C). This is attributed to the higher optical absorption by Te than CdTe. Finite-element simulations support the greater temperature rise in Te than CdTe when using a high TBR of $\sim 3.5 \times 10^{-7}$ m^2/KW between two materials, corresponding to the poor thermal contact. The laser-induced surface degradation of a CdTe sample depends on the initial surface properties of the sample. Therefore, determination of maximum laser power density to study Raman spectroscopy of CdTe without damaging its surface must be determined experimentally.

ACKNOWLEDGMENTS

S.S. and M.H. acknowledge partial support by the U.S. Department of Energy through Sunshot PVRD Grant DE-EE-0007541, "Crosscutting Recombination Metrology for Expediting V_{OC} Engineering."

[1]P. M. Amirtharaj and F. H. Pollak, Appl. Phys. Lett. **45**, 789 (1984).
[2]M. J. Soares and M. C. Do Carmo, Proc. SPIE Int. Soc. Opt. Eng. **4469**, 57 (2001).
[3]E. M. Larramendi, G. Berth, V. Wiedemeier, K.-P. Hüsch, A. Zrenner, U. Woggon, E. Tschumak, K. Lischka, and D. Schikora, Semicond. Sci. Technol. **25**, 075003 (2010).
[4]S. A. Hawkins, E. Villa-Aleman, M. C. Duff, D. B. Hunter, A. Burger, M. Groza, V. Buliga, and D. R. Black, J. Electron. Mater. **37**, 1438 (2008).
[5]L. C. Teague, S. A. Hawkins, M. C. Duff, M. Groza, V. Buliga, and A. Burger, J. Electron. Mater. **38**, 1522 (2009).
[6]V. Wiedemeier, G. Berth, A. Zrenner, E. M. Larramendi, U. Woggon, K. Lischka, and D. Schikora, Semicond. Sci. Technol. **26**, 105023 (2011).
[7]M. J. Soares, J. C. Lopes, M. C. Carmo, and A. Neves, Phys. Status Solidi C Conf. **1**, 278 (2004).
[8]E. Zielony, E. Placzek-popko, P. Kamyczek, A. Henrykowski, and G. Karczewski, Opt. Appl. **43**, 181 (2013).
[9]L. Burgio, R. J. H. Clark, and S. Firth, Analyst **126**, 222 (2001).
[10]K. Buckley and A. G. Ryder, Appl. Spectrosc. **71**, 1085 (2017).
[11]O. S. Ogedengbe *et al.*, J. Electron. Mater. **46**, 5424 (2017).
[12]S. Adachi, T. Kimura, and N. Suzuki, J. Appl. Phys. **74**, 3435 (1993).
[13]G. A. Kulkarni, V. G. Sathe, K. S. R. K. Rao, D. V. S. Muthu, and R. K. Sharma, J. Appl. Phys. **105**, 063512 (2009).
[14]A. Picos-Vega, M. Becerril, O. Zelaya-Angel, R. Ramírez-Bon, F. J. Espinoza-Beltrán, J. González-Hernández, S. Jiménez-Sandoval, and B. Chao, J. Appl. Phys. **83**, 760 (1998).
[15]B. K. Rai, H. D. Bist, R. S. Katiyar, K. T. Chen, and A. Burger, J. Appl. Phys. **80**, 477 (1996).
[16]H. R. Vydyanath, J. Ellsworth, J. J. Kennedy, B. Dean, C. J. Johnson, G. T. Neugebauer, J. Sepich, and P. Liao, J. Vac. Sci. Technol. B Microelectron. Nanom. Struct. **10**, 1476 (1992).
[17]H. R. Vydyanath, J. A. Ellsworth, J. B. Parkinson, J. J. Kennedy, B. Dean, C. J. Johnson, G. T. Neugebauer, J. Sepich, and P. K. Liao, J. Electron. Mater. **22**, 1073 (1993).
[18]H. N. Jayatirtha, D. O. Henderson, A. Burger, and M. P. Volz, Appl. Phys. Lett. **62**, 573 (1993).
[19]D. W. G. White, Metall. Mater. Trans. B **3**, 1933 (1972).
[20]S. Hunsche, K. Wienecke, and H. Kurz, Appl. Phys. A **62**, 499 (1996).
[21]S. Tutihasi, G. G. Roberts, R. C. Keezer, and R. E. Drews, Phys. Rev. **177**, 1143 (1969).
[22]M. Rothschild, C. Arnone, and D. J. Ehrlich, J. Mater. Res. **2**, 244 (1987).
[23]S. Lin, W. Li, Z. Chen, J. Shen, B. Ge, and Y. Pei, Nat. Commun. **7**, 10287 (2016).
[24]J. J. Alvarado, O. Zelaya-Angel, F. Sánchez-Sinencio, G. Torres-Delgado, H. Vargas, and J. González-Hernández, J. Appl. Phys. **76**, 7217 (1994).
[25]G. A. Slack, Phys. Rev. B **6**, 3791 (1972).
[26]Z. Liang and M. Hu, J. Appl. Phys. **123**, 191101 (2018).
[27]See supplementary material at https://doi.org/10.1116/1.5048526 for x-ray diffraction, atomic force microscopy and additional Raman spectroscopy results.